Supported Membranes: Scientific and Practical Applications

E. Sackmann*

Scientific and practical applications of supported lipid-protein bilayers are described. Membranes can be covalently coupled to or separated from solids by ultrathin layers of water or soft polymer cushions. The latter systems maintain the structural and dynamic properties of free bilayers, forming a class of models of biomembranes that allow the application of a manifold of surface-sensitive techniques. They form versatile models of low-dimensionality complex fluids, which can be used to study interfacial forces and wetting phenomena, and enable the design of phantom cells to explore the interplay of lock-and-key forces (such as receptor-ligand binding) and universal forces for cell adhesion. Practical applications are the design of (highly selective) receptor surfaces of biosensors on electrooptical devices or the biofunctionalization of inorganic solids.

Supported membranes on solids are of practical and scientific interest for several reasons. They enable biofunctionalization of inorganic solids (semiconductors, gold-covered surfaces, and optoelectronic devices) and polymeric materials. They provide a natural environment for the immobilization of proteins (such as hormone receptors and antibodies) under nondenaturing conditions and in a well-defined orientation. They allow the preparation of ultrathin, high-electric-resistance layers on conductors and the incorporation of receptors into these insulating layers for the design of biosensors based on electrical and optical detection of ligand binding.

Supported lipid-protein bilayers separated from the solid surface by nanometer-thick water layers or ultrathin soft polymer cushions maintain the thermodynamic and structural properties of free bilayers. This enables the application of several surface-sensitive techniques [microinterferometry, ellipsometry, surface plasmon spectroscopy, Fourier transform infrared (FTIR) spectroscopy, nuclear magnetic resonance (NMR), and neutron and x-ray surface reflectivity]. Such polymer membrane-composite films represent a class of low-dimensionality complex fluids that allow systematic studies of wetting phenomena under controlled humidity conditions and interfacial forces. Another attractive application of supported membranes is the design of phantom cells exhibiting well-defined adhesive properties and receptor densities, useful for study of the interplay of specific (lock-and-key) and universal forces during cell adhesion and locomotion on surfaces.

The author is in the Physik Department E22 (Biophysics Laboratory), Technische Universität München, D-85747 Garching, Germany. E-mail: sackmann@physik.tu-muenchen.de

*On leave at the Institute for Theoretical Physics, University of California, Santa Barbara, CA 93106, USA.

Self-Assembly and Manipulation of Supported Membranes

Three types of supported membranes can be assembled (Fig. 1): (i) integrated bilayers with the inner monolayer fixed to the substrate either covalently or by ion bridges (*1*, *2*), (ii) freely supported lipid-protein bilayers separated from the substrate by ultrathin water layers (~10 Å), and (iii) bilayer membranes resting on ultrathin, soft hydrated polymer films. A completely different type of supported membrane, used to immobilize monopolar (amphiphilic) proteins, can be formed by ultrathin polymer films (such as dextran) hydrophobized by coupling of long alkyl chains to the hydrophilic polymer backbone (Fig. 1C).

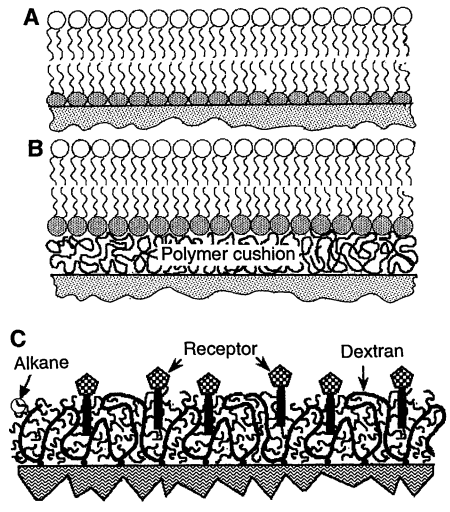

Fig. 1. Three types of supported membranes: (**A**) integrated membrane with covalently fixed inner monolayer, (**B**) supported bilayers separated from the substrate by ultrathin water films or polymer monolayers, and (**C**) ultrathin polymer film of hydrophobized macromolecules (dextran with alkane side groups) forming a cushion for monopolar receptors.

The common methods of membrane assembly on surfaces are monolayer transfer [by the Langmuir-Blodgett (LB) technique] and vesicle spreading. In both cases, the continuity (for example, as measured by electrical-impedance spectroscopy) of the supported membranes depends critically on the smoothness of the substrate. In order to separate membranes from the substrate by an ultrathin film of water, one must either treat the supports briefly by argon sputtering or use freshly cleaved mica (*2*). Integrated membranes are prepared by deposition of an alkyl monolayer as an inner layer by self-assembly from solution, with the use of alkyl silanes in the case of $Si\text{-}SiO_2$ supports and alkyl mercaptanes in the case of gold surfaces. Another method for integration of the first monolayer is coupling through salt bridges by the classical Kuhn technique (*3*).

Advantages of the subsequent monolayer transfer are that (i) the deposition process can be performed automatically, (ii) it may be followed optically by imaging ellipsometry or microfluorescence (*4*), and (iii) both layers can be manipulated in many ways. With the appropriate choice of lipid mixtures and thermodynamic conditions, monolayers of a multitude of different microscopic lateral organizations can be formed (*1*, *2*, *4*–*6*). The microstructure and packing density of the inner monolayer are conserved during the transfer but determine the structure and density of the outer layer. The latter solidifies over crystalline domains of the inner layer by epitactic coupling (*2*), unless its fluid-solid transition is far above ~20°C, the temperature of transfer. This condition enables the design of heterogeneously functionalized solid surfaces.

For vesicle spreading, the surface of the support has to be attractive or the vesicles must be under high tension, or both conditions may be needed (*7*). The bilayer may be linked electrostatically through ion bridges or covalently by lock-and-key forces (*8*). Two different mechanisms of vesicle spreading are possible (*9*) (Fig. 2, A and B): (i) the advancement of single bilayers with open edges and (ii) viscous fingerlike spreading of closed lobes of juxtaposed bilayers (protruding from giant vesicles) by means of a rolling motion of the upper bilayer over the substrate while the bilayer in contact with the substrate is immobilized by pinning centers. The former process prevails if the surface is strongly hydrated and

the bilayer and surface are separated by lubricating ultrathin water or polymer films (9). Only the latter process leads to closed bilayers by self-healing, whereas the former results in incomplete coverage.

Functionalization of Solid Surface and Supported Film

Functionalization of the solid surface is the key problem for the deposition of bilayers, the anchoring of polymers, and the direct immobilization of proteins on solid surfaces. Each system requires a different strategy. To anchor polymers (such as dextrans), one can deposit a mixed monolayer of long-chain surfactants exhibiting functional head groups (such as epoxy groups, amines, and nitrile groups) and alcohols (Fig. 3A). Alcohol groups render the surface hydrophilic and thus reduce nonspecific protein binding. For the direct immobilization of proteins on solids, an already classical method is to functionalize the surface with biotin-streptavidin layers and couple the proteins (such as antibodies) through biotin groups. The lateral anchor density can be controlled by depositing mixed monolayers with incorporated biotin-lipids (8).

The second problem is functionalizing the deposited membranes or polymer films. The simplest way is to incorporate monopolar receptors (such as proteins penetrating membranes only partially) into the bilayer. A more general strategy is to mediate protein coupling by active (succidinimide) esters (Fig. 3B), which are bound to the lipids or polymer chains, whereas the protein itself is coupled to the active ester through amine groups attached to the protein by spacers. This popular technique is well suited for the coupling of antigen epitopes or Fab fragments of antibodies to membranes [see (4) for further references].

An elegant way to reversibly couple proteins to supported membranes is based on chelating lipid (Fig. 3C). In the presence of bivalent ions (such as Ni^{2+} or Ca^{2+}), histidine oligomers bind to the chelator (10). The binding is completely reversible because the "receptor" can be detached by sequestering the bivalent ions with EDTA. The histidine tags of the proteins are attached by genetic engineering.

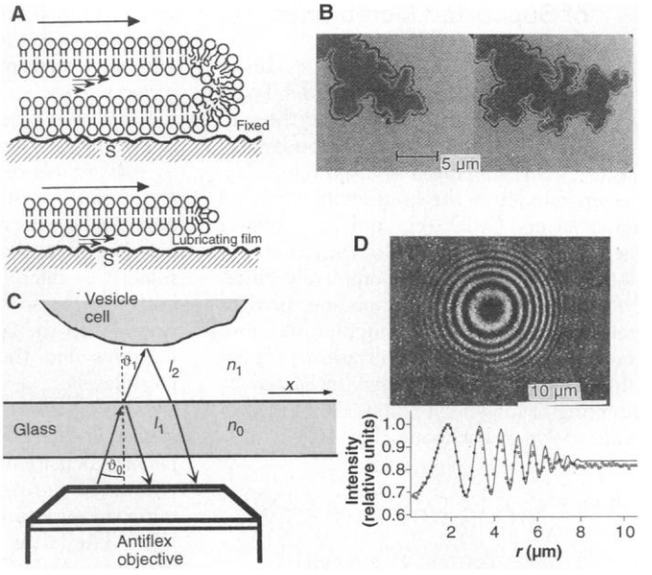

Fig. 2. (**A**) Two types of spreading of bilayers on substrates. Top shows viscous fingerlike spreading of a giant vesicle. Juxtaposed bilayers of lobes advance as the top bilayer rolls over the immobilized lower bilayer. Bottom shows spreading of single bilayer over a lubricating water film or polymer cushion. (**B**) RICM image of spreading lobes of juxtaposed bilayers by viscous fingering. (**C**) RICM images are formed by interference of light reflected from the substrate surfaces and the object. θ, incidence angles; *l*, lengths; and *n*, refractive indices. (**D**) By analyzing the interference pattern by dynamic image processing, one can reconstruct the surface profile and the average distance of the object surface from the solid with a resolution of ~5 nm in the normal and of ~0.3 μm in the lateral direction.

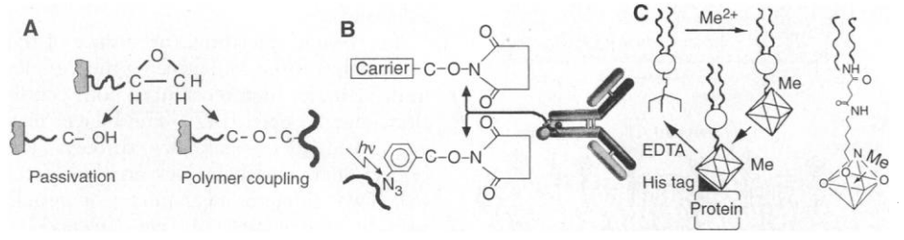

Fig. 3. (**A**) Functionalization of a solid surface with a mixed monolayer of surfactants (silanes, mercaptanes) carrying alcohol and functional groups. The alcohol groups passivate the surface, minimizing nonspecific binding of ligands, and the functional groups anchor the polymers. In the case of epoxy-group functionalization, some groups are transformed into OH by hydrolysis (which can be monitored by FTIR). Polymers are anchored to residual epoxy groups through COO^- groups. Another method of coupling is by photoaffinity labeling (through N_3 groups). (**B**) Irreversible coupling of proteins to membranes, polymer films, or solids through an active (succinimide) ester, as described in (4). (**C**) Reversible immobilization of proteins (exhibiting His tags) to supported membranes through chelating lipids. In the presence of bivalent ions (Ni^{2+}), proteins exhibiting protruding His sequences (≈3 His) bind but can be removed by EDTA.

Supported Bilayers: A Class of Model Membranes

Because supported membranes separated from the solid by ultrathin water or polymer films maintain the structural and thermodynamic properties of free lipid layers, their dynamic and structural properties can be studied by FTIR and NMR (6, 7), total internal reflection fluorescence (4, 11), surface scattering of x-rays and neutrons (6, 12), lateral diffusion measurements (Fig. 4) (4, 13), microoptical techniques such as imaging ellipsometry (14), and microinterferometry [reflection interference contrast microscopy (RICM) (9)]. Use of NMR spectroscopy of membranes deposited on spherical (glass or silica) beads allows one to avoid the many artifacts caused by polydispersity of the vesicle suspension and the local curvature effects that render data interpretation ambiguous (7).

Neutron reflectivity combined with contrast variation techniques provides a promising tool for the study of structural aspects of protein-membrane coupling (12) and protein-protein recognition processes at membrane interfaces. Experiments require only microgram quantities of protein, and radiation damage is avoided (in contrast to x-ray methods).

The RICM technique (Fig. 2, C and D) is a powerful tool for observing the dynamics of bilayer spreading (Fig. 2, A and B) and analyzing the two-dimensional (2D) organization of supported mono- and bilayers with a resolution of <5 Å in the normal and ≈0.3 μm in the lateral direction (9). The high azimuthal resolution of this 2D (optical) density mapping of supported films is achieved by contrast enhancement, realized by the deposition of a low refractive index layer (MgF_2 film 1/8 of a wavelength thick) on the solid support (9).

Lateral Diffusion at Interfaces Between Two and Three Dimensions

The most striking and biologically important consequences of the 2D fluid nature of lipid membranes is the logarithmic depen-

dence of the diffusion coefficient on the particle radius, as predicted by the Saffman-Delbrück model (*2*). This peculiar behavior enables large integral cell membrane proteins to diffuse nearly as fast as lipid molecules, as long as they are not coupled to the actin-cytoskeleton or embedded in immobilized domains (*13*). The situation is completely different for membranes in frictional contact with solid substrates, where the mobility of large diffusants (such as polymerized amphiphiles or proteins) is reduced by orders of magnitude compared to the lipid molecules (*2*, *13*). This slowing down of large molecules is a consequence of the frictional contact between the fluid bilayer and the solid support (Fig. 4), which generates two additional frictional forces. First, the velocity field induced by the diffusant in the membrane $\mathbf{v}_m$ leads to a frictional shear stress $\sigma_v = \eta_w \mathbf{v}_m/d_w$, where η_w is the viscosity of the lubricating film of thickness d_w. Second, a direct frictional force between the diffusant (of radius R) and the solid arises of the form $\mathbf{f}_{dir} = \pi R^2 b_{dir} \mathbf{v}_p = \pi R^2 \mathbf{v}_p \eta_w/d_w$ (b_{dir} = direct frictional coefficient measured in erg·s/cm^4, and $\mathbf{v}_p$ is the velocity of the particle). The total lateral frictional force (per square centimeter of membrane) is $\sigma = (b_s + b_{dir})\mathbf{v}_m = b_s^* \mathbf{v}_m$ ($b_s = \eta_w/d_w$). The diffusion coefficient may be expressed in terms of a dimensionless parameter $\epsilon \approx R\sqrt{b_s^* \eta_m^{(2)}}$ [see (*2*) for an exact expression]

$$D^{-1} = \frac{4\pi\eta_m^{(2)}}{k_B T}\left[\frac{1}{4}\epsilon^2 + \epsilon\frac{K_1(\epsilon)}{K_0(\epsilon)}\right] \quad (1)$$

where k_B is Boltzmann's constant, T is temperature, K_1 and K_0 are Bessel functions of the second kind, and $\eta_m^{(2)}$ is the 2D membrane viscosity, which is related to a bulk membrane viscosity $\eta_m^{(3)}$ (often called microviscosity) by $\eta_m^{(2)} = \eta_m^{(3)} d_m$. The second term in the bracket of Eq. 1 corresponds exactly to the classical Saffman-Delbrück logarithmic law, and the first accounts for the friction exerted by the wall. For thin lubricating films or large diffusing particles (such as proteins), the ϵ^2 term prevails and one obtains

$$D \approx \frac{k_B T}{\pi b_s^*} R^{-2} \quad (2)$$

Equation 2 can be applied to (i) measure the thickness of the lubricating films between solid and bilayer, (ii) measure radii of proteins or 2D hydrodynamic radii of polymerized amphiphiles (*13*), (iii) measure coefficients of friction between monolayers and their modification by solutes (*2*), and (iv) determine surface viscosities of ultrathin polymer films (*4*).

It is indeed hoped that systematic studies of the lateral diffusion of macromolecules embedded in bilayers that are deposited on soft polymer cushions will help clarify the not completely resolved problem of impeded protein diffusion in biomembranes [see (*4*, *13*) for further references]. The effect of partial coupling of proteins to cytoskeletons could be mimicked by the polymer film.

Integrated Membranes as Electrooptical Biosensors

The interest in supported membranes is strongly stimulated by their potential application to the design of biosensors. The basic idea (Fig. 5A) is to use the bilayer simultaneously (i) as a very thin electrical insulator, (ii) as a matrix for the incorporation of receptors (such as lipid-coupled antigens or antibodies), and (iii) for the suppression of nonspecific ligand binding. For electrical monitoring of ligand binding, the supports can consist of gold-covered or SnO_4/InO_4–covered supports or metal-oxide-semiconductor (field-effect transistors; MOSFETs), and ligand binding can be recorded by capacitance or current measurements.

The capacitance C_m of (supported) lipid-protein bilayers depends in a complex way on the dielectric constant and thickness d_m of the layer, the surface charge of the lipid bilayer and integrated proteins, and the distance between bilayer and support. The receptor surface may be characterized in terms of an effective (dielectric) thickness d_{eff}^{ϵ}. Ligand binding leads to a change in dielectric thickness of $\delta d_{eff}^{\epsilon} = \delta C_m/C_m^2$, indicating that very thin insulating layers are required to achieve high sensitivities.

Fortunately, the different contributions to the membrane impedance can be determined by analyzing the frequency dependence of the complex impedance Z_m of the membrane over a large range of frequencies (Fig. 5A). One convenient way is to measure the absolute value of Z_m and the phase shift Φ (Fig. 5B) and to simulate these so called "Bode plots" by assuming various equivalent circuits to decide which contributions C_i and R_i contribute and to determine the values of these parameters (*15*). Figure 5B shows, for example, that ignoring the capacitance of the defects C_d leads to very large discrepancies at low frequencies.

The sensitivity of the sensor based on impedance spectroscopy is mainly determined by the defect density. The total bilayer capacitance is $C_m = \Theta C_m^0 + (1 - \Theta) C_d$, where Θ is the surface coverage. Because the capacitance of the closed bilayer C_m^0 (~3 μF) is smaller than C_d (~30 μF) by an order of magnitude, the membrane capacitance is dominated by defects unless $\Theta > 0.97$ (*13*). The sensitivity achieved by electrical detection with such high-quality integrated membranes corresponds to 10^{11} receptors per square centimeter or to a minimum detectable mass of 10^{-9} g/cm^2.

The sensitivity could be improved in various ways. With FET transistors as measuring devices, the active sensor area could be reduced. More-sensitive devices could be used, such as the heterogeneous Si-Ge transistors (*16*), because the conductivity of these 2D electron conductors is extremely sensitive to changes in the surface charge. Another promising strategy is to use interdigitated arrays of microelectrodes with submicrometer electrode distances (*17*). To achieve sensitivities similar to enzyme-linked immunosorbent assays, one would have to develop enzymatic amplification

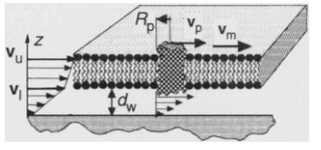

Fig. 4. Velocities and frictional coupling between opposing monolayers of membrane and between the inner monolayer and a rigid wall: $\mathbf{v}_p$, instantaneous velocity of the diffusing particle; $\mathbf{v}_m(z)$, the z-dependent velocity induced within the bilayer by the diffusant [changing from $\mathbf{v}_u$ to $\mathbf{v}_l$ (upper to lower)]; and d_w, thickness of the lubricating film. The velocity gradient in the lubricating film between the inner monolayer and the wall is v_l/d_w. Surface and bulk viscosities of polymer films can be measured by comparison of the diffusion of probes of different head-group structure (*2*, *4*).

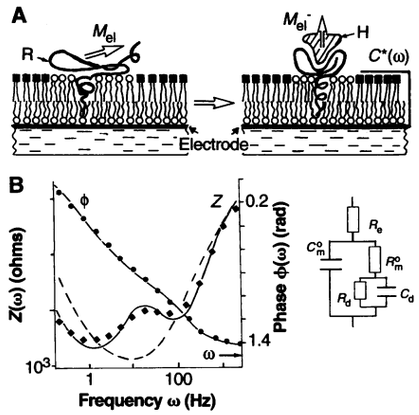

Fig. 5. Supported membranes as biosensors. (**A**) Detection of binding of ligand H to receptor R by complex capacitance (C^*) measurements (impedance spectroscopy). The capacitance C_m of the receptive layer is determined by its average thickness d_m and its dielectric constant ϵ_m, which depends on the electric dipole moment of receptor R (M_{el}, electric dipole moment of the head group of R). An effective electric thickness may be defined as $d_m^{el}/\epsilon_m = \epsilon_0 A/C_m$ (A = area of sensitive layer). (**B**) Evaluation of impedance spectra by equivalent circuits. Bode plots (data points) of frequency dependencies of absolute values of complex impedance Z^* and of the phase shift $\phi(\omega)$ (ω, angular frequency) over a large frequency regime are simulated by equivalent circuits (solid line). Dashed line shows large effect on $Z(\omega)$ if defect capacitance is ignored. R_e, resistance of the electrolyte.

mechanisms such as the activation of phospholipases (*15*) or of the complement systems. A completely different strategy would be to use immobilized cells as alarm systems (*18, 19*); however, the solid devices would have to be passivated by the deposition of membranes or ultrathin polymer films (Fig. 6) to avoid atrophy of the immobilized cells.

Another effective way to achieve signal amplification is to combine impedance spectroscopy with the more sensitive optical detection techniques, such as ellipsometry, surface plasmon resonance (SPR) (*20*), and surface acoustic wave techniques (*21*). The major advantage of impedance spectroscopy is its sensitive detection of nonspecific binding (*15*). Such tandem devices enable simultaneous multiparameter measurements in order to differentiate between different receptors or ligands. The introduction of SPR in the near infrared (1.3 to 1.8 μm), where both water and silicon exhibit absorption gaps, has enabled the combination of these techniques with silicon-based sensor devices (*21*). Natural combinations are SPR, impedance spectroscopy, and surface acoustic wave techniques, all of which require gold surfaces. Sensitivities achieved with these sensor devices correspond to thickness changes of 0.5 Å or 50 pg/mm^2.

One particular advantage of supported membranes as receptor surfaces is that the lateral distribution of membrane-bound (charged) ligands may be reorganized by 2D electrophoresis, as demonstrated for lipids (*22*). In principle, this allows for the separation of loaded and free receptors. Other possibilities are the enrichment of receptors over active areas of a device and the generation of lateral structures on nanometer scales.

A prerequisite for such manipulations of receptors is that the membrane and substrate must be separated by fully hydrated and soft polymer cushions. The cushions are expected to provide natural environments for the protein domains protruding from the bilayers.

Supported Membranes as Phantom Cells

Specific lock-and-key forces dominate the self-assembly on a molecular level (*23*) and play a central role for the modulation of allosteric enzyme activity by effectors (*24*) or immunological recognition processes. The interaction on a higher level of organization (such as between cells) is determined by a complex interplay of specific lock-and-key forces between receptors and a manifold of universal forces (Fig. 6). Besides the classical interaction mechanisms, these include polymer-induced forces (*25*) and dynamic repulsion forces (*26, 27*) caused by the thermally excited dynamic surface roughness of soft membranes.

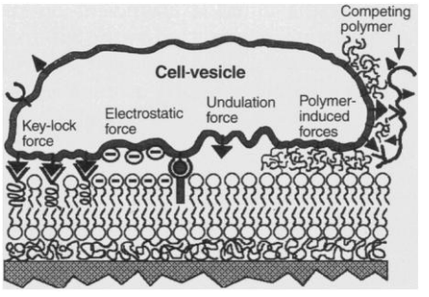

Fig. 6. Application of supported membranes as "phantom cells" to study the interplay of specific key-lock forces between receptors and universal forces. Incorporation of charged lipids, lipopolymers (or gangliosides), and receptors into supported bilayers allow control of electrostatic, polymer-induced, and lock-and-key forces. Dynamic repulsion forces caused by the dynamic surface roughness (resulting from membrane undulations and vibrational motion of lipid molecules in the normal direction) can be studied by observing the interaction of flickering cells (for example, erythrocytes) or vesicles with solid surfaces. The van der Waals forces can be varied by using solids of different Hamaker-constants or by separating membrane and solid by polymer cushions of various thicknesses.

Polymer-induced forces are repulsive if macromolecules are anchored to the interacting surfaces. If they can reversibly exchange between interfaces and bulk solutions, they may be repulsive at large or attractive at short interfacial separations (*25*). Another type of polymer-induced force arises if macromolecules compete with cells for binding sites on the substrate (Fig. 6).

The dynamic membrane roughness is determined by the local out-of-plane motions of lipids [amplitudes of 2 to 3 Å (*28*)] and thermally excited membrane undulations. The former contribute to repulsive short-range forces (~3 Å) together with the dehydration forces (*29*), whereas the latter lead to long-range entropic forces.

Supported membranes (and polymer films) open new possibilities for systematic studies of the interplay between specific and universal forces (for example, in cell adhesion). They enable the design of phantom cells with well-defined areal densities of (mobile and immobilized) receptors to control key-lock forces and allow subtle controls of universal forces (Fig. 6). Supported membranes have already been applied with great success to study the role of cell adhesion in immunological responses. It was shown that supported bilayers containing major histocompatibility complexes can replace antigen-presenting cells in order to study the interaction with T helper cells (*11*). Supported bilayers containing antigens coupled to lipids were applied to quantify the adhesion of T lymphocytes to membranes (*30*).

As an example, consider the measurement of undulation forces between vesicles and a solid wall. The energy (per unit area) associated with bending undulations is proportional to the square of the local curvature $H = (\partial^2 u/\partial x^2 + \partial^2 u/\partial y^2)$ generated by local deflections $u(x,y)$: $g_{bend} = \frac{1}{2}K_c H^2$ (Fig. 7). The bending modulus K_c (exhibiting the dimensions of energy) is $\sim 20 k_B T$ for natural lipids and may be even smaller ($\leq 5 k_B T$) in the presence of small amphiphiles (*31*). Thermal fluctuations can thus excite pronounced bending undulations with amplitudes of a few tenths of a micrometer. As a membrane approaches a hard wall, the undulations must be suppressed more and more because the mean amplitudes $\langle u \rangle$ of the undulations must be smaller than the average interfacial distance $\langle h \rangle$. Thus, a dynamic repulsive force or disjoining pressure results for entropic reasons (*26, 32, 33*).

Undulation forces can also play an important role in the control of cell adhesion. The best known example is the erythrocyte, which exhibits pronounced shape fluctuations called flickering (*34*), and there is evidence that the associated undulation forces prevent the sticking of cells to surfaces (such as that of the tissue), which may cause alterations of the cell surface and could accelerate the aging of cells. In most other cells, large-scale fluctuations of the lipid-protein bilayer of the plasma membrane are suppressed by coupling to the actin cortex of the cytoskeleton. However, on a local scale, the membrane is often decoupled from the cytoskeleton, resulting in small-scale undulations with wavelengths of the order of 0.5 μm and amplitudes of about 10 nm.

Detailed theoretical studies have shown (*33*) that the disjoining pressure P_{dis} depends critically on the lateral tension σ of the membrane. For $\sigma = 0$, it has the same dependence on $\langle h \rangle$ as the van der Waals potential between flat surfaces

$$P^0_{dis} = c' \frac{(k_B T)^2}{K_c \langle h \rangle^3} \quad (3)$$

where the constant c' is of the order of unity, whereas at $\sigma \neq 0$, an exponential law holds

$$P^\sigma_{dis} \approx \frac{k_B T \sigma}{4 \langle h \rangle K_c} \exp\left(-\frac{\pi \sigma}{3 k_B T} \langle h \rangle^3\right) \quad (4)$$

Detailed Fourier analysis of the undulations in the contact zone between the soft shell and the solid observed by RICM (*27*) allows the measurement for a single vesicle (or cell) of all of the essential parameters determining the undulation forces (Fig. 7). The van der Waals attraction may indeed be overcompensated by undulation forces at small tensions, resulting in a second minimum at a distance of ~100 Å (*27*). Thus,

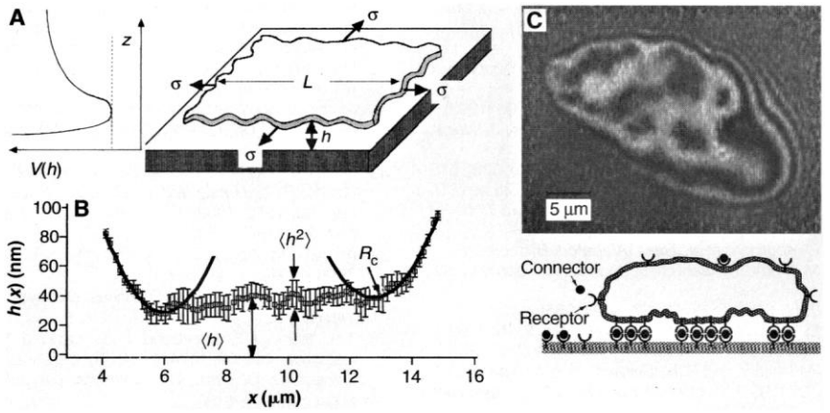

Fig. 7. Analysis of undulation forces between lipid vesicle and rigid wall. (**A**) Schematic view of a dynamically rough piece of membrane of dimensions L by L at distance h above the solid surface with lateral tension σ. The excitations may be decomposed into plane-wave Fourier modes. The effect of the wall is represented by an interfacial potential $V(h)$. (**B**) Representation of parameters characterizing weakly adhering vesicles simultaneously measurable by RICM. These include (i) mean distance $\langle h \rangle$ (~400 Å), (ii) mean square amplitude $\langle h^2 \rangle$ (~20 nm²), (iii) lateral tension ($\sigma \sim 0.001$ mN/m), (iv) force constant of potential $\partial^2 V/\partial Z^2$, (v) contract curvature R_c, and (vi) spatial correlation function of undulation amplitude $u(x)$ (*27*). (**C**) RICM visualization of a dimyristoyl phosphatidylcholine (DMPC) vesicle containing 1 mol % biotin-labeled lipid as the receptor interacting with a surface covered by streptavidin. The formation of adhesion plaques is caused by interplay of the strong attraction between receptors and the repulsive undulation forces.

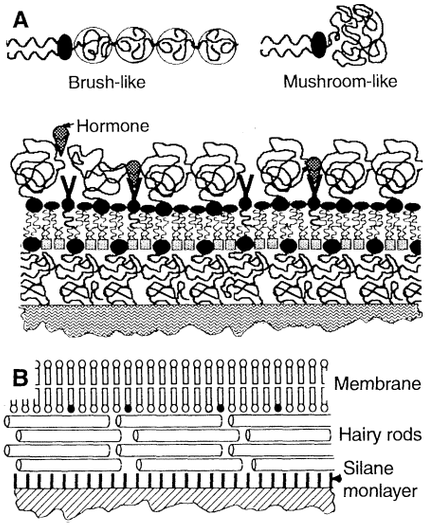

Fig. 8. (**A**) Separation of a bilayer from substrate by stealths formed by (clusters of) polymer brushes (or mushrooms) of hydrophilic polymers (for example, polyethyleneoxide grafted to long-chain lipids). Also shown is the formation of artificial glycocalix on the outer monolayer by the mixing of phospholipids, lipid-coupled receptors, and lipopolymers. (**B**) Membrane deposition on ultrathin layers of hairy rods prepared by the LB technique from hydrophobic hairy rods (cellulose-derivatives), which are hydrophilized by shaving of hydrophobic hairs in HCl vapor.

by increasing the tension, a transition from a weakly to a strongly bound state may occur and one may therefore speak of tension-induced adhesion (*33*). Transitions between free and bound states may arise if swelling is induced in vesicles or cells, leading to an increase of the lateral tension.

The remarkable strength of undulation forces is demonstrated in Fig. 7C. Vesicles containing ~1 mol % biotinylated lipid (as model "receptors") adhere to substrates covered with streptavidin to form tight binding sites. Although the specific attraction is very strong, only adhesive plaques form (dark patches), separated by strongly undulating regimes (bright patches). The latter are ~100 nm from the surface. This condensation of junctions can be understood on the basis of a recent theory by Bruinsma *et al.* (*35*). It arises if membranes are locally strongly coupled to another surface through specific short-range forces (such as those mediated by receptors) but exhibit simultaneously a repulsive long-range disjoining pressure (such as that caused by electrostatic repulsion or undulation forces). This effect may play a role in the formation of gap junctions between cells or the formation of focal adhesion plaques during, for example, the strong adhesion of fibroblasts to surfaces.

Polymer-Lipid Composite Films: A Perspective

Composite polymer-lipid films open new perspectives for (i) the reconstitution of membrane-spanning proteins and the reorganization or local enrichment of receptors by 2D electrophoresis (isoelectric focusing), (ii) fundamental studies of the mobility of membrane proteins coupled to macromolecular networks, and (iii) the deposition of self-healing (defect free) membranes to increase the electric resistivity and suppress nonspecific binding (Fig. 5). Composite monolayer-polymer films are also versatile model systems for studies of fluid-fluid wetting by viscous fingering or solitary waves (*14*) as well as dewetting processes. To mimick the physical properties of cytoskeletons beneath cell plasma membranes (such as the spectrin-actin network of erythrocytes), the polymer cushions must be soft and fully hydrated, which excludes highly charged polyelctrolytes (such as polylysine) or strongly cross-linked gels as supporting cushions.

The key problem is that the stability of these soft asymmetric films is determined by two stability criteria. First, the spreading coefficient $S = \gamma_{pw} - \gamma_{pm} - \gamma_{mw}$ must be positive, where γ_{pw}, γ_{pm}, and γ_{mw} are the free energies per unit area of the polymer-water, polymer-membrane, and membrane-water interfaces, respectively. For soft polymers, for which water is a very good solvent, this condition is in general difficult to fulfill (*14*). Second, the membrane-substrate interaction must be repulsive or only weakly attractive in order to prevent dewetting. This condition is difficult to fulfill for monolayers on polymer cushions (*14*).

One successful strategy is to make the inner monolayer of lipopolymers grafted to the head groups, which serve as pillars to keep the bilayer 30 to 100 Å from the support (Fig. 8A). The distance can be varied by means of the lateral pressure because the polymer can be switched between the stretched (brush-like) and more expanded (mushroom-like) conformations (*36*). Lipopolymers in the outer monolayer allow one to synthesize artificial glycocalices to study the influence of steric repulsion on cell-substrate interactions or the accessibility of ligands to receptors and to minimize nonspecific binding effects (*37*). Supported membranes that are separated from the surface of gold-covered substrates by hydrophilic spacers have been prepared by the deposition of polymerized amphiphiles with thiol groups coupled to the polymer backbone or by transfer of bilayers of lipids carrying thiol head groups (*38*).

A second successful strategy is to form polymer cushions from multilayers of hairy rods prepared by the LB technique (Fig. 8B) (*39*). In fact, ultrathin meshworks can be formed by partial cross-linking of the rods exhibiting voids for integral protein penetration. Dextran films anchored to glass substrates by the technique of Fig. 3 also fulfill most of the requirements mentioned above (*40*).

REFERENCES AND NOTES

1. H. M. McConnell, L. K. Tamm, R. M. Weiss, *Proc. Natl. Acad. Sci. U.S.A.* **81**, 3249 (1984).
2. R. Merkel, E. Sackmann, E. A. Evans, *J. Phys. France* **50**, 1535 (1989); E. A. Evans and E. Sack-

mann, *J. Fluid Mech.* **194**, 553 (1988).
3. H. Kuhn, H. D. Möbius, H. Bücher, *Physical Methods of Chemistry*, Part IIIB, A. Weissenberger and B. M. Rossiter, Eds. (Wiley, New York, 1972).
4. M. Egger, S. P. Heyn, H. E. Gaub, *Biophys. J.* **57**, 669 (1990); M. Kühner, R. Tampé, E. Sackmann, *ibid.* **67**, 217 (1994); E. Kalb, S. Frey, L. K. Tamm, *Biochim. Biophys. Acta* **1103**, 307 (1992).
5. T. H. Watts and H. M. McConnell, *Ann. Rev. Immunol.* **5**, 461 (1987).
6. A. Fischer, M. Lösche, H. Möhwald, E. Sackmann, *J. Phys. Lett.* **45**, 785 (1984); H. Möhwald, *Annu. Rev. Phys. Chem.* **41**, 441 (1990).
7. Th. M. Bayerl and M. Bloom, *Biophys. J.* **58**, 357 (1990).
8. R. Blankenburg, P. Meller, H. Ringsdorf, C. Salesse, *Biochemistry* **28**, 8214 (1989); W. Müller *et al.*, *Science* **262**, 1706 (1993).
9. J. Rädler and E. Sackmann, *J. Phys. II France* **3**, 727 (1993); T. Feder, G. Weissmüller, B. Zeks, E. Sackmann, *Phys. Rev. E* **51**, 3427 (1995); J. Rädler, H. Strey, E. Sackmann, *Langmuir*, in press.
10. L. Schmitt, C. Dietrich, R. Tampé, *J. Am. Chem. Soc.* **116**, 8485 (1994).
11. T. H. Watts, H. Gaub, H. M. McConnell, *Nature* **320**, 179 (1986); H. M. McConnell, T. H. Watts, R. M. Weis, A. A. Brian, *Biochim. Biophys. Acta* **864**, 95 (1986).
12. C. A. Helm, H. Möhwald, K. Kjaer, J. AlsNielsen, *Europhys. Lett.* **4**, 697 (1983); S. J. Johnson *et al.*, *Biophys. J.* **59**, 289 (1991); Th. Bayerl and E. Sackmann, in *Cholesterol and Membrane Models*, L. Finegold, Ed. (CRC Press, Boca Raton, FL, 1992).
13. P. Eggl, D. Pink, B. Quinn, H. Ringsdorf, E. Sackmann, *Macromolecules* **23**, 3472 (1990); P. F. F. Almeida and W. C. C. Vaz, in *Handbook of Biological Physics*, vol. 1, R. Lipowsky and E. Sackmann, Eds. (Elsevier, Amsterdam, 1995).
14. G. Elender and E. Sackmann, *J. Phys. II France* **4**, 455 (1994).
15. M. Stelzle, G. Weissmüller, E. Sackmann, *J. Phys. Chem.* **97**, 2974 (1993); G. Brink, L. Schmitt, R. Tampé, E. Sackmann, *Biochim. Biophys. Acta* **1196**, 227 (1994).
16. G. Abstreiter, *Phys. Scr.* **T49**, 42 (1993).
17. U. Wollenberger, M. Paeschke, R. Hintsche, *Analyst* **119**, 1245 (1994).
18. H. M. McConnell *et al.*, *Science* **257**, 1906 (1992).
19. P. Fromherz, A. Ofennhausser, T. Vetter, J. Weiss, *ibid.* **252**, 1290 (1991).
20. B. Rothenhäusler and W. Knoll, *Nature* **332**, 615 (1988); M. M. S. Löfas, I. Rönneberg, E. Senberg, B. Liedberg, I. Lundström, *Sens. Actuators B* **5**, 79 (1991).
21. C. Kößlinger *et al.*, *Sens. Actuators B*, in press.
22. M. Stelzle, R. Miehlich, E. Sackmann, *Biophys. J.* **63**, 1346 (1992).
23. J.-M. Lehn, *Science* **227**, 849 (1985).
24. D. E. Koshland, *Trends Biochem. Sci.* **9**, 155 (1984).
25. P. de Gennes, *Macromolecules* **15**, 492 (1982).
26. W. Helfrich and R. M. Servuss, *Nuovo Cimento D* **3**, 137 (1994); R. Lipowsky and S. Leibler, *Phys. Rev. Lett.* **56**, 2541 (1986).
27. J. Rädler, T. Feder, H. Strey, E. Sackmann, *Phys. Rev. E* **51**, 4526 (1995).
28. S. König, W. Pfeiffer, T. Bayerl, D. Richter, E. Sackmann, *J. Phys. II France* **2**, 1589 (1992); J. Israelachvili and H. Wennerstroem, *Langmuir* **6**, 873 (1990).
29. V. A. Parsegian, N. Fuller, R. P. Rand, *Proc. Natl. Acad. Sci. U.S.A.* **76**, 2750 (1979).
30. A. Toezeren *et al.*, *J. Cell Biol.* **116**, 997 (1992).
31. H. P. Duwe, J. Käs, E. Sackmann, *J. Phys. France* **51**, 945 (1990).
32. The two-dimensional (2D) gas model of dynamically rough surfaces: Because the undulations are statistically excited and strongly overdamped, the lipid bilayer exhibits a random surface and may be considered a 2D analog of a semiflexible coil. The undulations are characterized by a mean square amplitude $\zeta_\perp^2 = \langle u^2 \rangle$ ($\zeta_\perp$ is called the roughness coefficient) and a lateral correlation length $\zeta_\parallel$ characterizing the lateral range over which the orientations of the local membrane normals are correlated [$\langle n(r)n(0) \rangle \propto \exp(-r/\zeta_\parallel)$]. Following Helfrich (*26*), the fluctuating bilayer may thus be considered as a 2D gas composed of a flat pieces of dimension $\zeta_\parallel^2$ that fluctuate in the normal direction with amplitudes $\zeta_\perp^2$ exhibiting thermal energies $\frac{1}{2}k_BT$. The disjoining pressure (energy per unit volume) is of the order $P_{dis} \approx k_BT/\zeta_\parallel^2\,\zeta_\perp$. The roughness coefficient and correlation length are related by $\zeta_\perp = \sqrt{k_BT/K_c}\cdot\zeta_\parallel$, and because $\zeta_\perp \leq \langle h \rangle$, Eq. 3 for P_{dis} results.
33. U. Seifert and R. Lipowsky, *Phys. Rev. A* **42**, 4768 (1991); R. Lipowsky and B. Zielinska, *Phys. Rev. Lett.* **62**, 1572 (1989); E. A. Evans and W. Rawicz, *ibid.* **64**, 2094 (1990).
34. A. Zilker, M. Ziegler, E. Sackmann, *Phys. Rev. A* **46**, 7998 (1992).
35. R. Bruinsma, M. Goulian, P. Pincus, *Biophys. J.* **67**, 746 (1994).
36. T. L. Kuhl, D. E. Leckband, D. D. Lasic, J. N. Israelachvili, *ibid.* **66**, 1474 (1994); Th. Beackmark, G. Elender, D. D. Lasic, E. Sackmann, *Langmuir*, in press.
37. D. Needham, T. McIntosh, D. D. Lasic, *Biochim. Biophys. Acta* **1108**, 40 (1992).
38. J. Spinke, J. Yang, J. Wolf, M. Liley, H. Ringsdorf, W. Knoll, *Biophys. J.* **63**, 167 (1992); H. Lang, C. Duschl, H. Gratzel, H. Vogel, *Thin Solid Films* **210**, 818 (1992).
39. G. Wegner, *Thin Solid Films* **216**, 105 (1992).
40. E. Sackmann *et al.*, unpublished results.
41. I thank T. Feder for providing the unpublished results on adhesion. This article was written during a fruitful sojourn at the Institute for Theoretical Physics of the University of California, Santa Barbara, supported in part by the National Science Foundation under grant PHY89-04035. I gratefully acknowledge the hospitality of J. S. Langer and the staff of the institute and enlightening discussions with many visitors of the Biomembrane Program of 1994. I thank P. Pincus and S. C. Safinya for the invitation to this program. Much of the work is based on a year-long cooperation with H. Ringsdorf and his group.